Int J Adv Manuf Technol (2016) 82:2017–2028
DOI 10.1007/s00170-015-7530-3

ORIGINAL ARTICLE

Experimental study of tool life transition and wear monitoring in turning operation using a hybrid method based on wavelet multi-resolution analysis and empirical mode decomposition

Mohamed Khemissi Babouri[1,2] · **Nouredine Ouelaa**[1] · **Abderrazek Djebala**[1]

Received: 7 April 2015 / Accepted: 1 July 2015 / Published online: 15 July 2015

Abstract This paper deals with the experimental study of the tool life transition and the wear monitoring during the turning operation of AISI D3 steel workpiece using coated carbide tool inserts ($TiCN/Al_2O_3/TiN$). A hybrid method, based on the combination of wavelet multi-resolution analysis (WMRA) and Empirical Mode Decomposition (EMD), is proposed to analyze vibratory signals acquired during the machining process. Using the mean power and the energy as main scalar indicators, the proposed method has been optimized and evaluated in several configurations including the cutting speed, the feed rate, and the depth of cut. The results show that the proposed hybrid method (WMRA/EMD) gives better evaluation of the tool state and the wear monitoring compared to the application of WMRA or EMD alone.

Keywords Vibration signal · Tool wear · Intrinsic mode function · Wavelet transform · Empirical mode decomposition

Nomenclature

A_j	Approximations
a_p	Depth of cut, mm
D_i	Details
E	Energy
EMD	Empirical mode decomposition
F	Feed rate, mm/rev
F_S	Sampling frequency
IMFs	Intrinsic mode functions
P_m	Mean power
Ra	Arithmetic mean roughness, μm
Rt	Total roughness, μm
Rz	Mean depth of roughness, μm
T	Cutting time, s
VB	Flank wear, mm
V_c	Cutting speed, m/min
WMRA	Wavelet multi-resolution analysis

✉ Abderrazek Djebala
djebala_abderrazek@yahoo.fr

Mohamed Khemissi Babouri
babouri_bmk@yahoo.fr

Nouredine Ouelaa
n_ouelaa@yahoo.fr

[1] Mechanics and Structures Laboratory (LMS), May 8th 1945 University, Po. Box 401, 24000 Guelma, Algeria

[2] Department of Mechanical Engineering and Productics (CMP), FGM & GP, University of Sciences and Technology, Houari Boumediene, Po. Box 32, El-Alia Bab-Ezzouar 16111, Alger, Algeria

1 Introduction

Monitoring cutting tool's wear via vibration analysis has long been practiced, modern methods are only more sophisticated extensions of the earliest investigations. Recent technological advances, particularly in signal processing, have made the acquisition and the analysis of vibratory signals a useful tool for monitoring the degradation state of the cutting tool. This degradation affects the quality of the machined surfaces, the imposed geometrical tolerances, the tool behavior, and generates high forces. One of the serious consequences of a not controlled and brutal wear is the stop of the cutting process, causing the breakage of the tool and the mobile bodies of the machine, and consequently the productivity fall. Numerous methods have been proposed for the tool wear monitoring, these methods are based on the analysis of various physical quantities; acoustic emission, cutting forces or vibration signals that can be detected by machining, by direct control of the cutting tool, or by estimating its state [1–5].

In the literature, Mer and Diniz [6] carried out experiments for correlating the variation of the tool vibration, tool wear, tool life, and surface roughness in the finish turning operation using coated carbide tools. Dimla [7] described a good cutting tool condition monitoring system in a metal turning operation using vibration features. The monitoring revealed that the vibration signals features are related to the wear qualification of the cutting tool. Das et al. [8] have demonstrated the interest of measuring the cutting force and the feed force to the force of repression. The magnitude of the cutting force and the feed force increases significantly with the development of the cutting tool wear, while the magnitude of the force discharge remains almost constant. Haili et al. [9] studied the rupture of a turning tool by analyzing the acoustic emission signals in time and time-frequency domains. The tool breakage is clearly detectable and is characterized by a significant increase in the amplitude. Ravindra et al. [10] developed a methodology for detecting the flank wear through the study of the acoustic signal spectrum. It has been shown that the RMS value of the measured signal is sensitive to the tool state. It reduces in the phase of break-in, remains stable in the stabilization phase, and increases significantly in the phase of accelerated wear. This parameter has the same behavior under different cutting conditions chosen in this study. This address the limits of the spectral analysis, time-frequency methods, namely wavelet analysis, enables a local view of the signal instead of the Fourier analysis that gives only global view. Several applications of the wavelet analysis for the tool wear prediction have been proposed in continuous and discrete versions [11, 12]. Some other applications proposed an automatic detection using different architectures of neural networks [13, 14].

Wavelets being non-adaptive, however, have its own disadvantage that their analysis results depend on the choice of the wavelet base function. The empirical mode decomposition is a new method proposed as a legitimate successor of the wavelet analysis. EMD is a self-adaptive decomposition of the signal; any complex signal can be decomposed into several intrinsic mode functions (IMF) representing the natural oscillatory modes embedded into the signal [15].

The aim of this paper is to identify the tool life transition and then to detect the rupture of the cutting edge in its earliest state using coated carbide tool during aggressive machining of AISI D3 steel. The vibratory signals measured during the machining are then processed by wavelet multi-resolution analysis (WMRA), empirical mode decomposition, and a hybrid method based on the combination of the two mentioned methods (WMRA/EMD).

2 Cutting tools monitoring

The cutting tool life represents the actual productive time during which the cutting edge is directly related to wear. The wear manifests itself on the cutting tool in several forms dependent of the cutting conditions, the material being machined, the material of the cutting tool and its geometry. In normal cutting conditions, flank wear (VB) is considered to assess the dominant wear of the cutting tool life [16]. The development of this type of tool wear is not a random phenomenon. In practice, and also theoretically, the flank wear (VB) follows the pattern represented by Fig. 1 and presents three wear phases: (A) Break-in phase, (B) Wear stabilization, and (C) Accelerated wear.

The device of cutting tool monitoring allows the measurement of a representative signal of the tool state, the treatment of this signal, and the detection of possible anomaly. To this end, the good choice of a data measurement and processing device is essential for an on line monitoring system of the cutting tools. This treatment is made according to the sensor and the quality of the taken signals. The extraction of useful information built-in in these signals is carried out by analysis or by filtering; this allows identification of the tool life transition.

2.1 Wavelet multi-resolution analysis theory

The wavelet transform is a mathematical transformation which represents a signal $s(t)$ in term of shifted and dilated version of singular function called wavelet mother $\psi(t)$. This can be written mathematically by [17]:

$$\int_{-\infty}^{+\infty} \psi(t)dt = 0 \tag{1}$$

$$\psi_{a,b}(t) = \frac{1}{\sqrt{a}}\psi\left(\frac{t-b}{a}\right) \tag{2}$$

With a and b the scale and the translation parameters, respectively.

Noting by $\psi^*(t)$ the conjugate of $\psi(t)$, the continuous wavelet transform (CWT) of the signal $s(t)$ is defined by:

$$\mathrm{CWT}(a,b) = \frac{1}{\sqrt{a}}\int_{-\infty}^{+\infty} s(t)\psi^*\left(\frac{t-b}{a}\right)dt \tag{3}$$

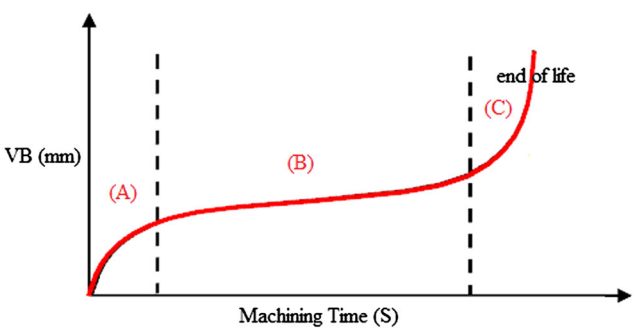

Fig. 1 Theoretical tool wear

A practical version of this transform, called wavelet multi-resolution analysis (WMRA), was introduced for the first time by Mallat in 1989 [18]. He had the idea to consider the wavelet analysis as a decomposition of the signal by a waterfall of filters, associating a pair of filters in each level of resolution (Fig. 2). The decomposition consists to introduce the signal $s(t)$ in low-pass (L) and high-pass (H) filters. In this level, two vectors will be obtained, cA1 and cD1. The elements of the vector cA1 are called approximation coefficients, they correspond to the low frequencies of the signal, while the elements of the vector cD1 are called detail coefficients and they correspond to the highest of them. The process of decomposition can be repeated n times, with n the number of levels. During the decomposition, the signal $s(t)$ and vectors cAj undergo a downsampling, this is why the approximation cAj and detail cDj coefficients pass through two new reconstruction filters (LR) and (HR). Two vectors result; Aj called approximations and Dj called *details*.

2.2 Empirical mode decomposition theory

The technique of empirical mode decomposition is a recent signal processing method. It allows breaking up any signal into a series of oscillating components extracted directly from this one in an adaptive way. In other words, EMD method is developed from the simple assumption that any signal consists of different simple intrinsic modes of oscillations. Each mode should be independent of the others. In this way, each signal could be decomposed into a number of IMFs. These IMFs components are interpreted like non-stationary forms of waves. This method has been used in several works [19–23]. IMF is an innovation concept proposed by Huang and his colleagues in Empirical Mode Decomposition, which is defined as a function that satisfies the following definition [24]:

1. In the whole data set, the number of extrema and the number of zero-crossings must either equal or differ at most by one;
2. At any point, the mean value of the envelope defined by local maxima and the envelope defined by the local minima is zero;

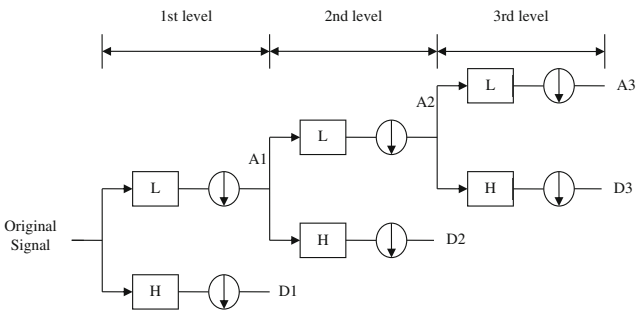

Fig. 2 Waterfall decomposition at three levels

The IMF represents the simple oscillation mode involved in the signal $s(t)$. Empirical mode decomposition is a sifting process used to extract the IMFs as follow (Table 1). To clarify the decomposition processes, Fig. 3 shows the procedure of EMD.

3 Experimental procedure

3.1 Material

The material used in this study is steel with high chromium content designated by AISI D3. It has an excellent behavior with wear and applied for the manufacture of matrices, punches blanking, stamping, drawing die, rollers profilers and wood tools, and combs for nets rolling. Its chemical composition (in wt%) is given as follows: 2 % C, 11.50 % Cr, 0.30 % Mn, 0.25 % Si and 0.70 % Tun. Some physical properties of AISI D3 are given as follows: density 7.7 kg/m^3; elastic modulus 21.10 MPa, and thermal conductibility 20 W/m °C. The workpieces are used in the form of round bars having 80 mm and 300 mm in diameter and in length, respectively. The machining experiments were performed under dry conditions using a conventional lathe type SN 40C with 6.6 kW spindle power.

3.2 Cutting tool and tool holder

Coated carbide inserts of International Organization for Standardization (ISO) geometry SNMG 120408-MF 2015 manufactured by Sandvik are used throughout the investigation. The CVD coating is a multilayer of TiCN/Al_2O_3/TiN formed on a cemented carbide substrate. It consists of a thick, moderate temperature (MT) CVD of TiN for heat resistance and providing low friction coefficient. Despite the fact that TiCN offers a good resistance to wear and thermal stability,

Table 1 EMD Algorithm

(1) Initialize : $r_0=x(t)$, and $i=1$;
(2) Extract the ith IMF
(2.1) Initialize: $h_{i(k-1)}=r_i$, $k=1$
(2.2) Identify the local extrema and minima of $h_{i(k-1)}$
(2.3) Interpolate the local extrama and the minima by cubic spline lines to from upper and lower envelopes
(2.4) Designate the mean $m_{i(k-1)}$ of upper and low envelopes
(2.5) *Let* $h_{i(k-1)}-m_{i(k-1)}=h_{ik}$
(2.6) If h_{ik} becomes an IMF then IMFi=h_{ik}, go to step (2.2) with $k=k+1$
(3) Define $r_i - IMFi=r_{i+1}$
(4) At the end of the decomposition process we have a residue r_n and a collection of n IMFs, c_i ($i=1,2,\ldots,n$). is finished and r_{i+1} is the residue of the signal.
(5) Summing up all IMFs and the final residue r_n, we obtain :
$x(t)=\sum_{i=1}^{n} c_i + r_n$

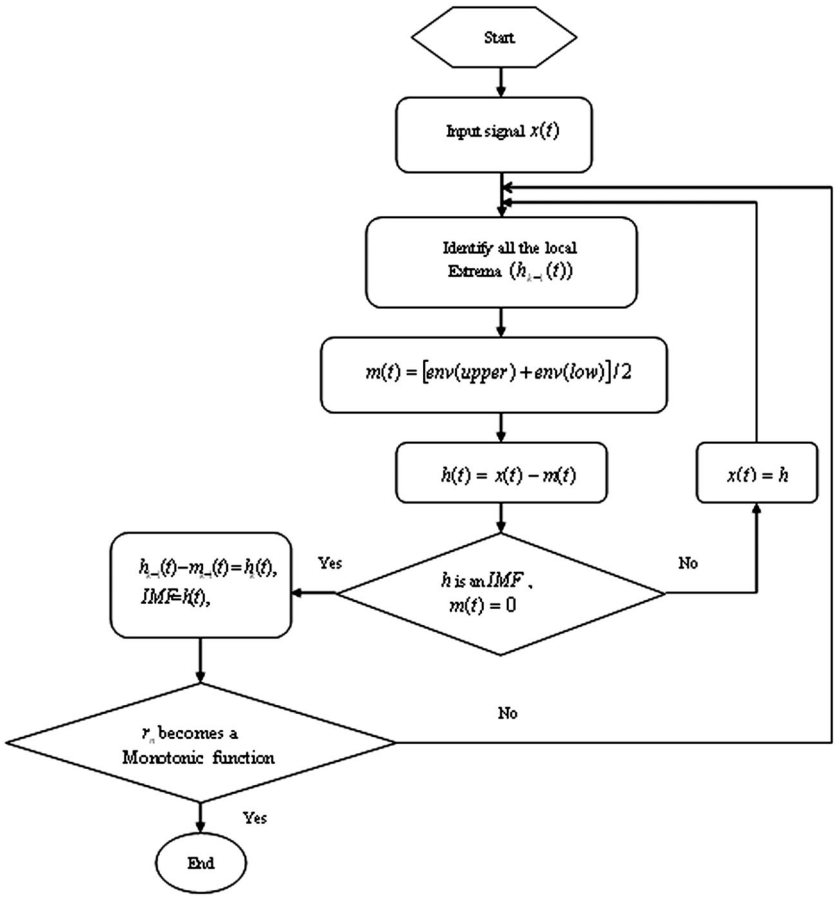

Fig. 3 Flow chart for empirical mode decomposition (EMD)

a layer of Al_2O_3 is required to bear effects resulting from high-temperature conditions, hot hardness, and crater wear damage. By now, it is well confirmed that this combined top coating and associated gradient substrate confer excellent behavior during dry machining [25]. The ISO tool holder reference is PSDNN 2525 M12 and the tool geometry is characterized as follows: χ=+75°; α=+6°; γ=−6° and λ=−6°.

3.3 Measurement setup

The components of the acceleration signals acquired throughout 116 s are measured on three channels (x, y, z), the setup used in the experiments is schematically shown by Fig. 4. The acquisition of the signals generated during machining was carried out using a 4524B Brüel & Kjaer type triaxial accelerometer, which makes it possible to record the acceleration in real time in the three principal directions for a sampling frequency of 32768 Hz, each measured signal contains 16,384 samples. Collected data was stored directly on the PC hard drive by the Pulse Lab shop® software. The increase of the cutting insert wear is measured after each machining pass by a Visual 250 type optical microscope (optical magnification: 0.7×4.5×actual size) using the Visual Gage software. Quickly and accurately this software is also distinguished by its ease of use, graphical interface and flexibility when creating measurement reports. The measurement is performed by placing the wafer on a micrometer cross table, a digital display is performed on the graphical interface. After each test, the cutting insert is dismounted from the tool carrier and cleaned. It is finally placed on the table of the microscope to measure the flank wear from the new to the end state of the tool life. A 2D Surftest 301 Mitutoyo type roughness meter was used to measure the three surface roughness (Ra, Rt, and Rz). It consists of a diamond point (probe) with a 5 mm radius and moves linearly on the working surface. Roughness values were obtained without disassembling the workpiece in order to reduce uncertainties due to resumption operations. The measurements are repeated three times on the surface of the workpiece at three reference lines equally positioned at 120°, and the final result is an average of these values. The experimental results are given in Table 2. For each cutting condition, four types of responses are recorded.

4 Tool life transition and wear study

4.1 Vibratory responses for wear monitoring

Statistical study was conducted by machining workpieces with three inserts from the same batch. The machining tests

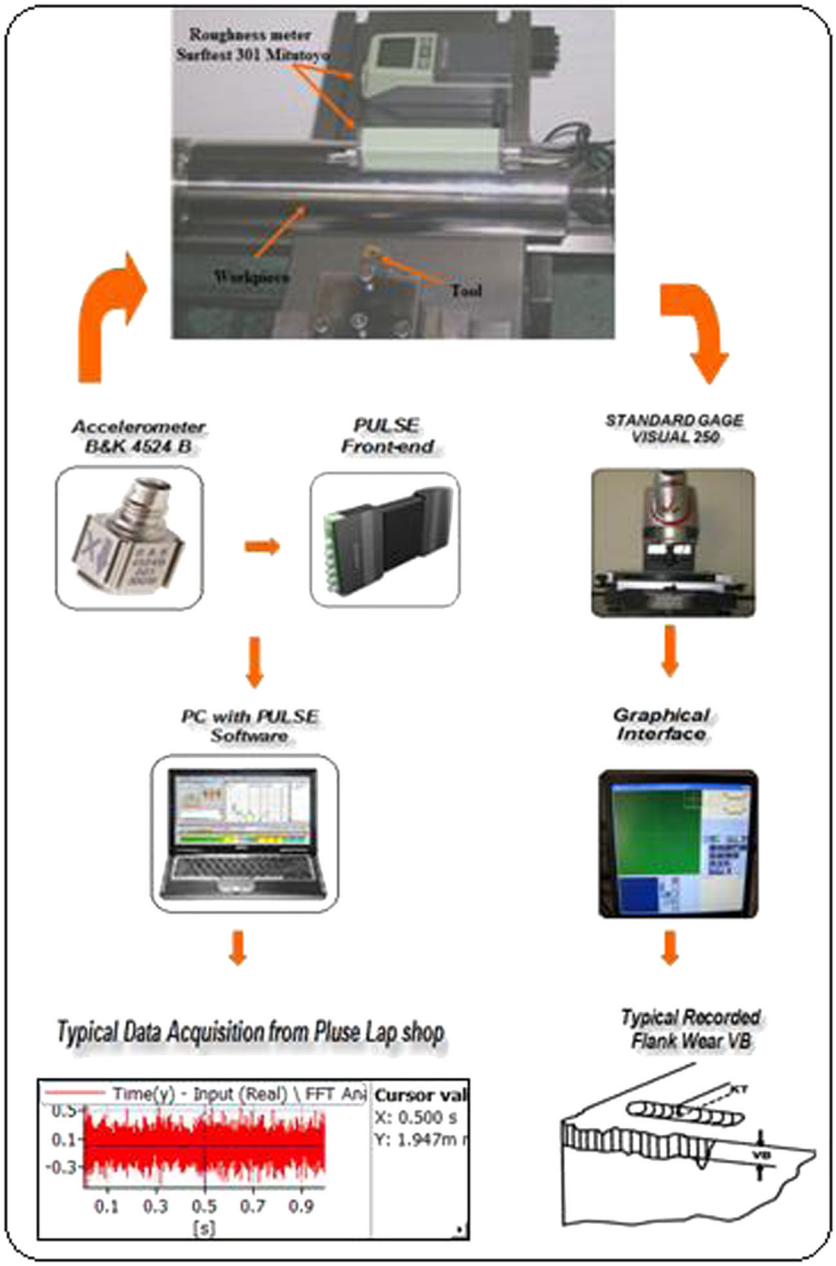

Fig. 4 Experimental setup

Table 2 Experimental data for AISI D3

	Tool life (s)	Wear (mm)	Roughness (μm)		
Runs	T	VB	R_a	R_t	R_z
V_c=175 m/min, a_p=0.2 mm, f=0.12 mm/rev					
1	116	0.077	0.48	4.12	3.52
2	348	0.289	1.54	7.96	7.82
3	464	0.373	2.49	11.21	10.53
4	580	0.488	2.76	12.61	11.46
5	696	0.628	5.23	20.19	19.63
V_c=250 m/min, a_p=0.2 mm, f=0.12 mm/rev					
1	116	0.091	0.80	4.01	4.00
2	232	0.218	1.21	6.45	6.24
3	348	0.359	3.06	12.82	12.50
4	464	0.920	7.90	35.99	34.62

were performed without lubrication and stop when flank wear reaches or exceeds the value of 0.3 mm, which is synonymous of tool lifespan. At this value, the cutting insert is in the wear acceleration phase corresponding to a critical zone of the machining quality.

Figure 5 shows an example of a concatenation of the vibration acceleration signals over the entire service of the cutting tool life. According to this figure, it is observed that there are three principal phases of the tool life: break-in period, wear stabilization, and accelerated wear where its rate increases until the rapid aging of the tool occurs. In particular, the transition to the acceleration phase is certainly detectable in the radial direction, this observation is the same on all

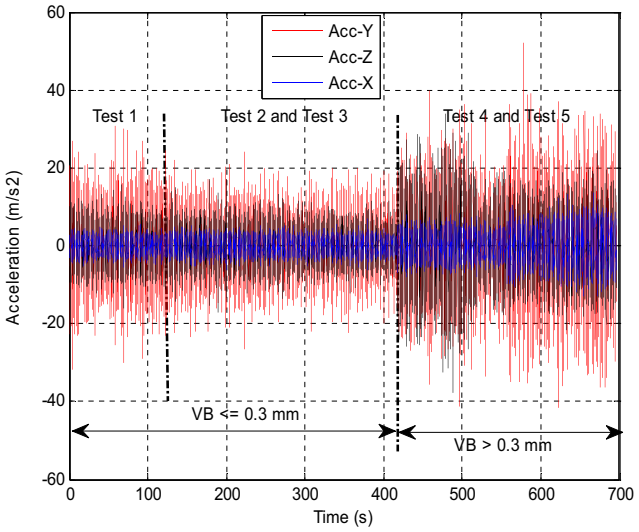

a) $V_c = 175$ m/min; $f = 0.12$ mm/rev; $a_p = 0.2$ mm

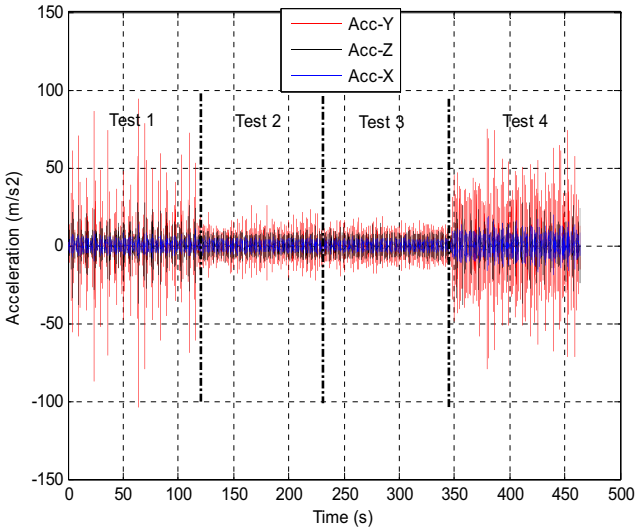

b) $V_c = 250$ m/min; $f = 0.12$ mm/rev; $a_p = 0.2$ mm

Fig. 5 Concatenation of signals over all the tool life of four and five vibratory answers

acquisitions. The analysis tends to enable the detection of the transition point from the stabilization phase to the accelerated wear phase. The importance of determining this transition point is fundamentally linked to the beginning of aging before the total collapse of the cutting tool.

4.2 Evolution of roughness and flank wear (VB)

The characterization of the quality of the machined surface has been limited to the criteria of arithmetic mean roughness (Ra), total roughness (Rt), and mean depth of roughness (Rz). The results of the roughness as a function of wear shows that the increase of flank wear degrades the quality of the machined surface. It should be noted here that, as irregular wear does not exceed the permissible value VB=0.3 mm, surface roughness (Ra) changes very slowly and the surface state is acceptable. Beyond this value, the roughness undergoes an abrupt increase.

Table 2 shows that for a cutting speed of 175 m/min the flank wear regularly develops between 0.077 mm (Ra= 0.48 μm) and 0.289 mm (Ra=1.54 μm) before expanding with time reaching a value of 0.373 mm and Ra=2.49 μm. One can also note at the end of the trial and after 11 min of machining that a collapse has formed on the tool nose with a wear VB=0.620 mm and Ra=5.23 μm. This latter is due to thermo-mechanical stresses on the tip of the tool, which shows the cutting high-temperature abrasive power causing rapid tool wear.

At 250 m/min within 2 min of machining, the insert undergoes an accelerated wear caused by temperature increase, chipping is observed on the rake surface. After 8 min with VB=0.920 mm, small collapse of the tool nose is noted. Machining lasted with chipping on the rake surface that propagates along the diagonal direction of the insert. Grooves, resulting from high abrasive wear, are also located while wear VB is generating on tool flank. At this stage, the increase in cutting speed raises the friction and the deformations and consequently the temperature in the cutting zone. Mechanical and thermal stresses on the cutting edge increase and lead to a catastrophic failure. The machining in these cutting conditions becomes unstable; it is accompanied by the increase in vibration, which returns it almost impossible and led to restrict the range of cutting speed.

During the tests, the machine is stopped constantly and the flank wear on each insert is evaluated according to the procedure recommended by ISO 8688-1. The experimental results of the morphology of the flank wear are shown in Fig. 6. For a cutting speed of 175 m/min, at the beginning, there was no difficulty in machining, the wear on flank surface is regular. When increasing the machining time, after

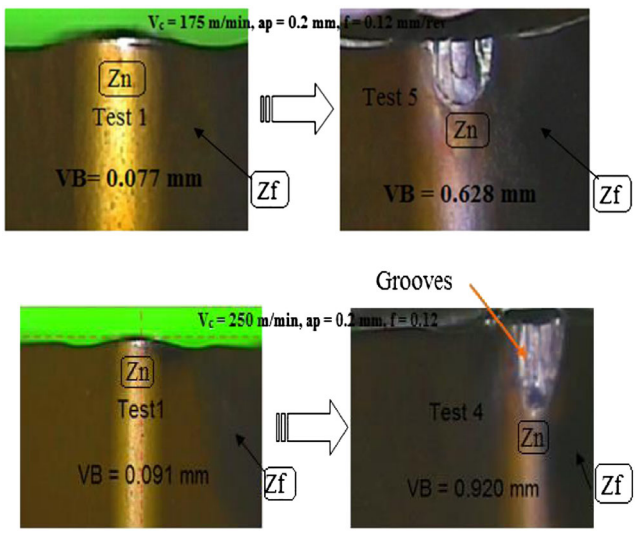

Fig. 6 Progression of flank wear (*Zn* insert nose zone, *Zf* flank face zone)

11 min, the wear VB expands in width and increases to becoming irregular with VB=0.628 mm. Chippings are observed on the tool rake surface following the high stresses generated from the cutting process. The rapid evolution of VB and KT led to the collapse of the tool nose. This collapse has the effect of increasing the roughness of the machined surface and affects the dimensional accuracy. The analysis of these results shows that the cutting speed has a major influence on wear.

5 Tool wear monitoring using hybrid method WMRA/EMD

Several researchers proposed the combination of several methods, on one hand to compare them, and on the other hand to amalgamate the sources of information. In this context, the wavelet multi-resolution analysis is first used as a pretreatment of the signal to be analysed. The empirical mode decomposition is then applied on the filtered signal obtained by WMRA. The suggested approach is that the application of the EMD on a signal previously filtered by WMRA provides better results than its application on the original signal. The procedure of the proposed approach is summarized as shown in the flowchart of Fig. 7.

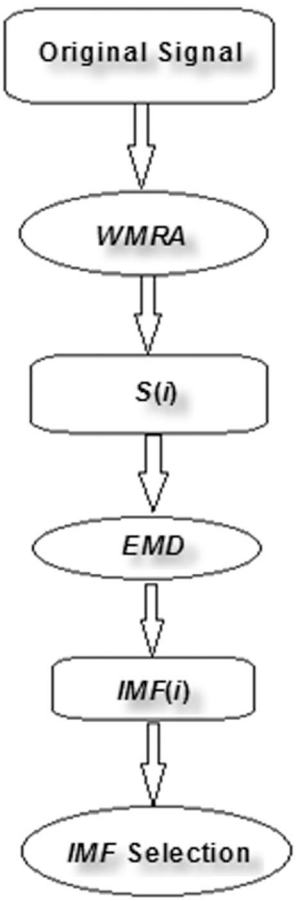

Fig. 7 Chart for the proposed method

The energy and the mean power are used as optimisation and evaluation criteria. The energy of a signal S with N samples is given by:

$$E = \sum_{k=1}^{N} S_k^2 \tag{4}$$

The mean power is defined by [26]:

$$P_m = \frac{F_s}{N} \sum_{k=1}^{N} S_k^2 \tag{5}$$

Where Fs is the sampling frequency.

5.1 Choice of the optimal decomposition signal of the WMRA

Using the waterfall algorithm, the measured signal is decomposed by the WMRA into several details, corresponding to the high frequencies, and the approximations corresponding to the lowest of them. The details are actually narrow band signals, the question to be asked is which detail is the optimal one. Figure 8 represents an acceleration signal and its decomposition using WMRA on four levels. Daubechies (db5) wavelet is used as analyzing function. The mean power and the energy values of each decomposition vector are calculated; Fig. 9 shows the obtained results for two cutting speeds.

It is easy to note that the highest values are obtained for the detail 1 (D1). That means that the concentration of the vibratory energy is present in this detail. For this reason it will be considered as the optimal decomposition vector, called reconstructed signal. The same results are obtained using other scalar indicators, like the RMS and the peak value, which confirms the assumption put before.

Moreover Fig. 10 shows the FFT spectrum of the detail (D1) considered as the reconstructed signal. The spectrum

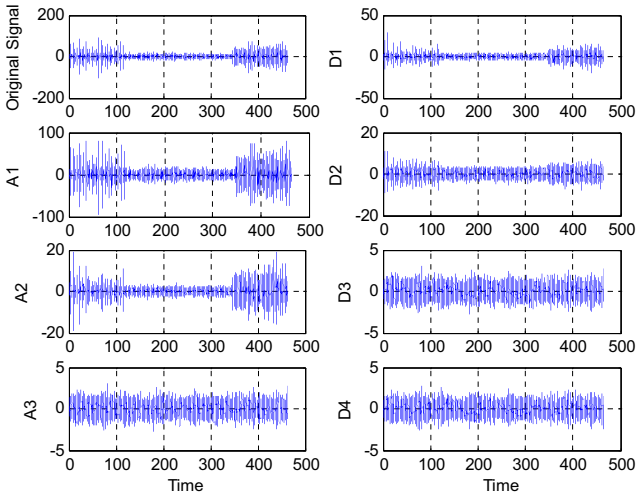

Fig. 8 Acceleration signal and its decomposition using WMRA

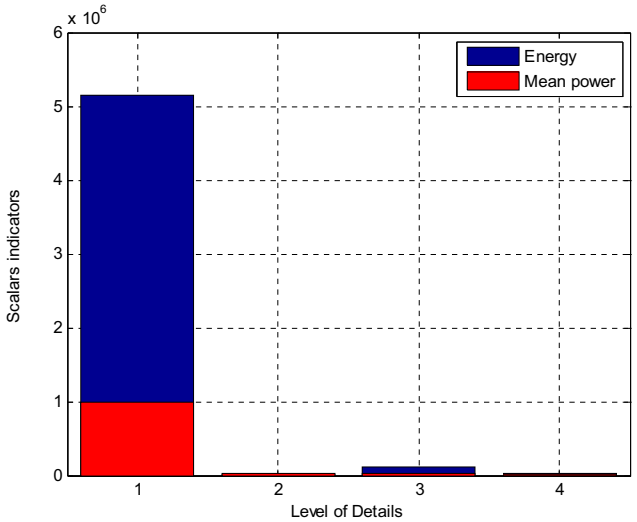

Fig. 9 Mean power and energy values of each decomposition vector

shows that the frequency band of the detail (D1) covers the tool's natural mode appearing in the band 3500–5500 Hz that has been previously identified by modal analysis. In our previous investigations, it has been shown that the tool's natural frequency is the principal component allowing the monitoring of the tool's wear (the best frequency indicator) [27].

5.2 Choice of the optimal Intrinsic Mode Function of the EMD

It has been shown in section (3.2) that the Empirical Mode Decomposition approach decomposes the signal into several Intrinsic Mode Functions (IMF). Obviously, only the first three IMFs are the real components of the signal and the others are the pseudo-components that have low frequency and will be represented as low-frequency components. Therefore, the

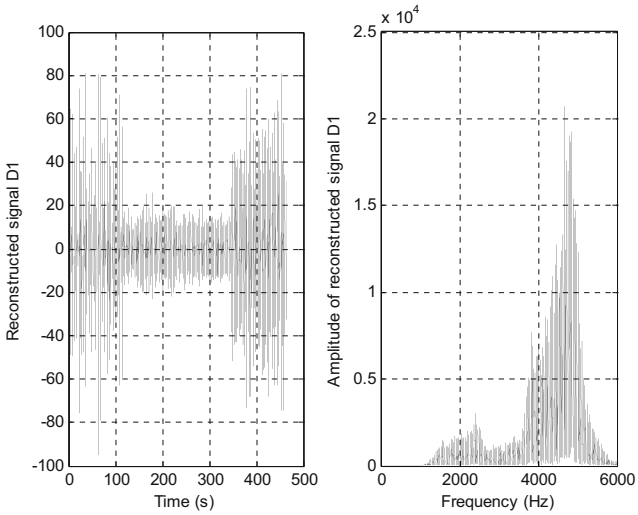

Fig. 10 FFT spectrum of the detail D1

first IMFs are true signal components and have relative good correlation with the original signal, whereas the other components are in the pseudo-low-frequency range and have only poor correlation.

To confirm this, the same approach applied for the optimal choice of the wavelet decomposition vector is used here. Figure 11 represents an acceleration signal and its decomposition by EMD method in 15 IMFs and the residue (just the first five and the latest IMFs are presented). Figure 12 represents the energy and the mean power for the first four IMFs, it shows that the IMF1 has the highest values for the two considered cutting speeds. For this reason, it will be considered as the optimal one. Since the IMF1 is a high-frequency component of the signal and the more representative one, its spectrum covers the tool's natural frequency previously identified by modal analysis and by the spectrum of the detail (D1) of the WMRA (Fig. 13).

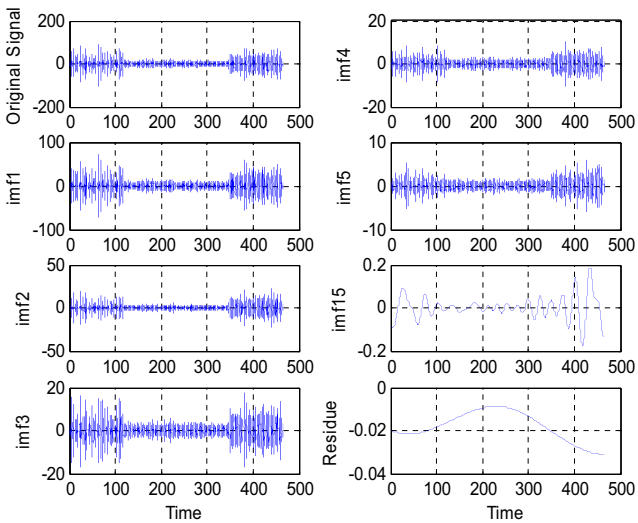

Fig. 11 Acceleration signal and its decomposition by EMD method at V_c=250 m/min; f=0.12 mm/rev; a_p=0.2 mm

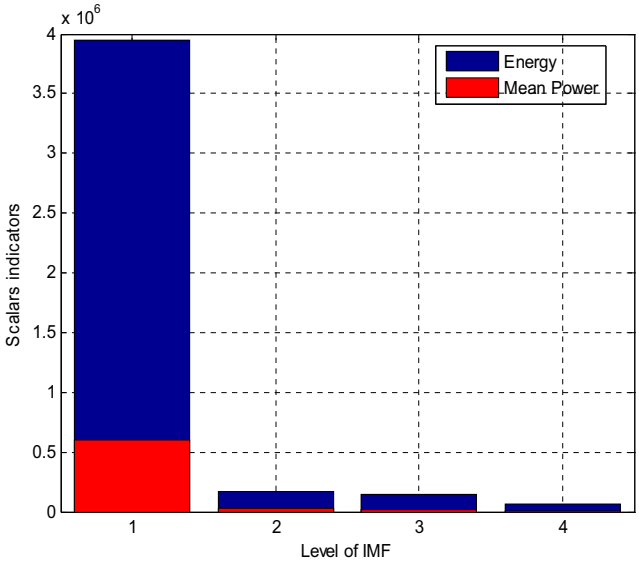

a) V_c = 175 m/min; f = 0.12 mm/rev; a_p = 0.2 mm

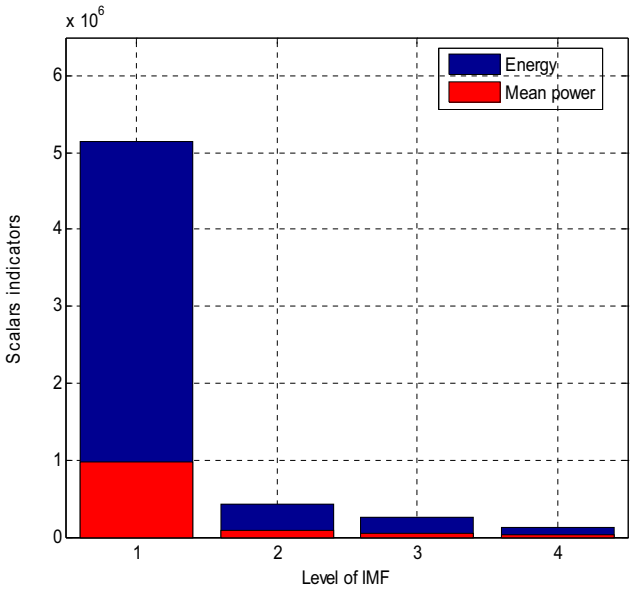

b) V_c = 250 m/min; f = 0.12 mm/rev; a_p = 0.2 mm

Fig. 12 Energy and mean power for the first four IMFs

Moreover, it is very interesting to note that the variation of the energy and the mean power of the IMF1 according to the wear (VB) has the same variation than that of the theory, the three wear phases are clearly identified. For the cutting speed V_c=250 m/min (Fig. 14), one can note that in the first phase, the energy is equal to 1.580E+06 for VB=0.091 mm. In the second phase of wear stabilization, it decreases and remains almost constant and equal to 3.59E+05 for VB=0.359 mm, before increasing one more time in the last phase corresponding to the wear acceleration reaching 3.26E+06 for VB=0.92 mm. The same findings are observed for the mean power.

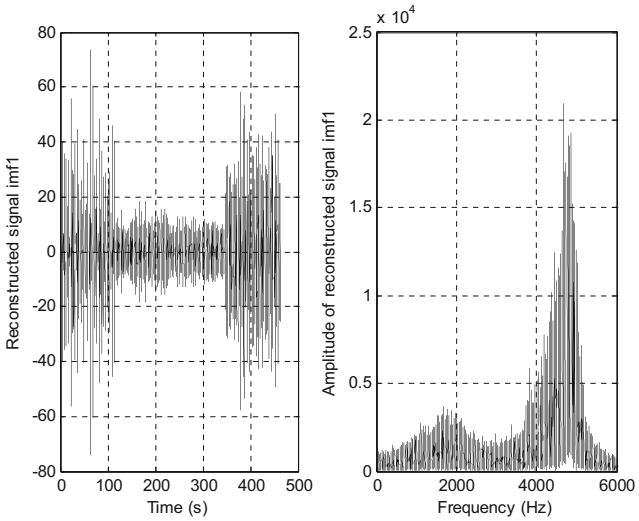

Fig. 13 FFT spectrum of the IMF1

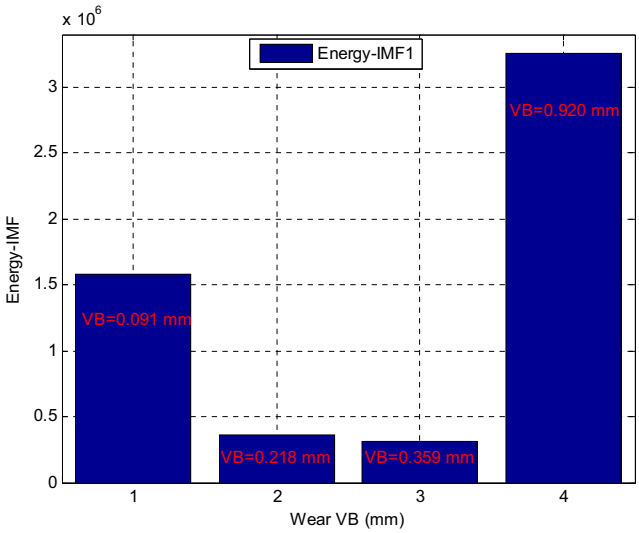

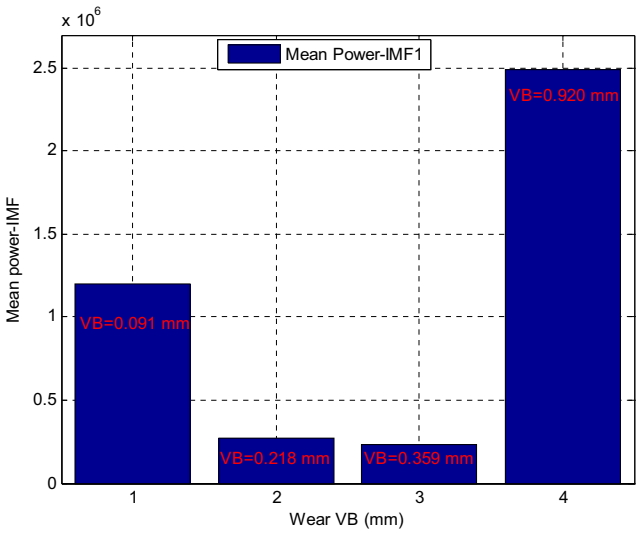

Fig. 14 Variation of the energy and the mean power of the IMF1 according to the wear (VB) at V_c=250 m/min; f=0.12 mm/rev; a_p= 0.2 mm

Table 3 Scalar indicators for V_c=175 m/min

Tool life (s)	Scalar indicators							
	Original signal		WMRA		EMD		Proposed method	
	Energy	M. Power	Energy	M. Power	Energy	M. Power	Energy	M. Power
8.718	3.945E+5	6.019E+5	3.787E+6	5.778E+5	3.787E+6	5.778E+5	4.131E+6	6.304E+5
26.13	3.671E+6	5.602E+5	3.548E+6	5.413E+5	3.548E+6	5.413E+5	3.809E+6	5.812E+5
52.27	4.046E+6	6.174E+5	3.905E+6	5.959E+5	3.905E+6	5.959E+5	4.174E+6	6.368E+5
87.11	3.961E+6	6.044E+5	3.829E+6	5.843E+5	3.829E+6	5.843E+5	4.140E+6	6.318E+5
122.0	3.214E+6	4 .904E+5	3.075E+6	4.690E+5	3.075E+6	4.691E+5	3.326E+6	5.076E+5
148.1	2.789E+6	4.256E+5	2.634E+6	4.020E+5	2.630E+6	4.020E+5	2.850E+6	4.348E+5
217.8	2.508E+6	3.980E+5	2.450E+6	3.738E+5	2.450E+6	3.738E+5	2.668E+6	4.071E+5
270.0	2.449E+6	3.737E+5	2.323E+6	3.544E+5	2.323E+6	3.544E+5	2.495E+6	3.807E+5
322.3	1.833E+6	2.796E+5	1.690E+6	2.579E+5	1.690E+6	2.579E+5	1.821E+6	2.779E+5
348.3	1.899E+6	2.897E+5	1.780E+6	2.716E+5	1.780E+6	2.716E+5	1.923E+6	2.934E+5
409.3	1.335E+6	2.037E+5	4.165E+6	1.849E+5	1.212E+6	1.849E+5	1.309E+6	1.997E+5
453.0	6.797E+6	1.037E+6	6.597E+6	1.007E+6	6.597E+6	1.007E+6	7.111E+6	1.085E+6
496.5	7.163E+6	1.093E+6	6.930E+6	1.057E+6	6.930E+6	1.057E+6	7.459E+6	1.138E+6
557.5	8.121E+6	1.239E+6	7.368E+6	1.124E+6	7.368E+6	1.124E+6	7.842E+6	1.197E+6
670.7	9.664E+6	1.475E+6	8.894E+6	1.357E+6	8.894E+6	1.357E+6	9.585E+6	1.463E+6

5.3 Obtained results

Tables 3 and 4 represent the energy and the mean power calculated for the entire tool life for a cutting speed of 175 and 250 m/min, respectively. These indicators are calculated for the original signal, and the signals reconstructed from WMRA, EMD, and the proposed hybrid method WMRA/EMD. For the cutting speed 175 m/min (Table 3), the WMRA and the EMD alone give almost the same results and which remain not significant since the scalar indicators have not been improved compared to those of the original signal. Whereas the proposed hybrid method shows weak

Table 4 Scalar indicators for V_c=250 m/min

Tool life (s)	Scalar indicators							
	Original signal		WMRA		EMD		Proposed method	
	Energy	M. Power	Energy	M. Power	Energy	M. Power	Energy	M. Power
7.260	8.990E+4	1.715E+4	6.643E+6	1.267E+6	6.840E+6	1.305E+6	6.971E+6	1.330E+6
21.78	1.331E+4	2.538E+4	1.211E+7	2.309E+6	1.214E+7	2.316E+6	1.246E+7	2.377E+6
43.56	8.396E+4	1.601E+4	6.889E+6	1.314E+6	7.183E+6	1.370E+6	7.156E+6	1.365E+6
65.34	1.077E+6	2.054E+4	8.921E+6	1.702E+6	8.944E+6	1.706E+6	9.280E+6	1.770E+6
108.9	1.025E+5	1.955E+4	9.761E+6	1.862E+6	9.925E+6	1.893E+6	1.014E+7	1.935E+6
152.5	4.807E+4	9169	1.357E+6	2.589E+5	1.367E+6	2.607E+5	1.491E+6	2.844E+6
210.5	3.605E+4	6875	1.824E+6	3.479E+5	1.866E+6	3.559E+5	1.965E+6	3.749E+5
261.4	4.104E+4	7828	1.437E+6	2.740E+5	1.462E+6	2.789E+5	1.571E+6	2.996E+5
312.2	3.907E+4	7451	1.305E+6	2.488E+5	1.346E+6	2.567E+5	1.438E+6	2.743E+5
334.0	3.889E+4	7418	1.134E+6	2.163E+5	1.137E+6	2.169E+5	1.260E+6	2.404E+5
348.5	6.170E+5	1.177E+5	1.090E+7	2.078E+6	1.004E+7	1.914E+6	1.149E+7	2.191E+6
377.5	7.989E+5	1.524E+5	1.522E+7	2.902E+6	1.468E+7	2.799E+6	1.588E+7	3.029E+6
406.6	6.027E+5	1.149E+5	1.337E+7	2.551E+6	1.333E+7	2.543E+6	1.377E+7	2.626E+6
421.1	1.135E+6	2.165E+5	1.414E+7	2.696E+6	1.424E+7	2.716E+6	1.482E+7	2.826E+6
450.1	7.608E+5	1.451E+5	1.315E+7	2.507E+6	1.310E+7	2.498E+6	1.380E+7	2.633E+6

improvement of the scalar indicators compared to those of the original signal and those obtained from WMRA and EMD alone. For the cutting speed 250 m/min (Table 4), the scalar indicators have been improved using WMRA and EMD, and especially using the proposed hybrid method that gives the highest results. It can be noted that the application of the proposed method for high cutting speeds gives better results.

On the other hand, Fig. 15 shows the evolution of the scalar indicators (energy and mean power) for the original signal and the reconstructed signal obtained from the proposed hybrid method over the entire tool life. Besides the improvement of the scalar indicator values ensured by the hybrid method, the three wear periods are clearly shown in this case. It is very easy to locate the break-in period until 120 s of machining, the wear stabilization period from 120 to 340 s, and finally the wear acceleration zone from 340 s. For the original signal, the variation of the same scalar indicators do not allows locating clearly the three zones, especially the transition from the break-in to the wear stabilization which seem as the same zone.

6 Conclusion

This paper presents an experimental study of the tool life transition and wear monitoring using hybrid method based on wavelet multi-resolution analysis and empirical mode decomposition. Vibratory signals have been measured during dry turning of steel workpieces (AISI D3) using coated carbide tool inserts ($TiCN/Al_2O_3/TiN$). The measured signals

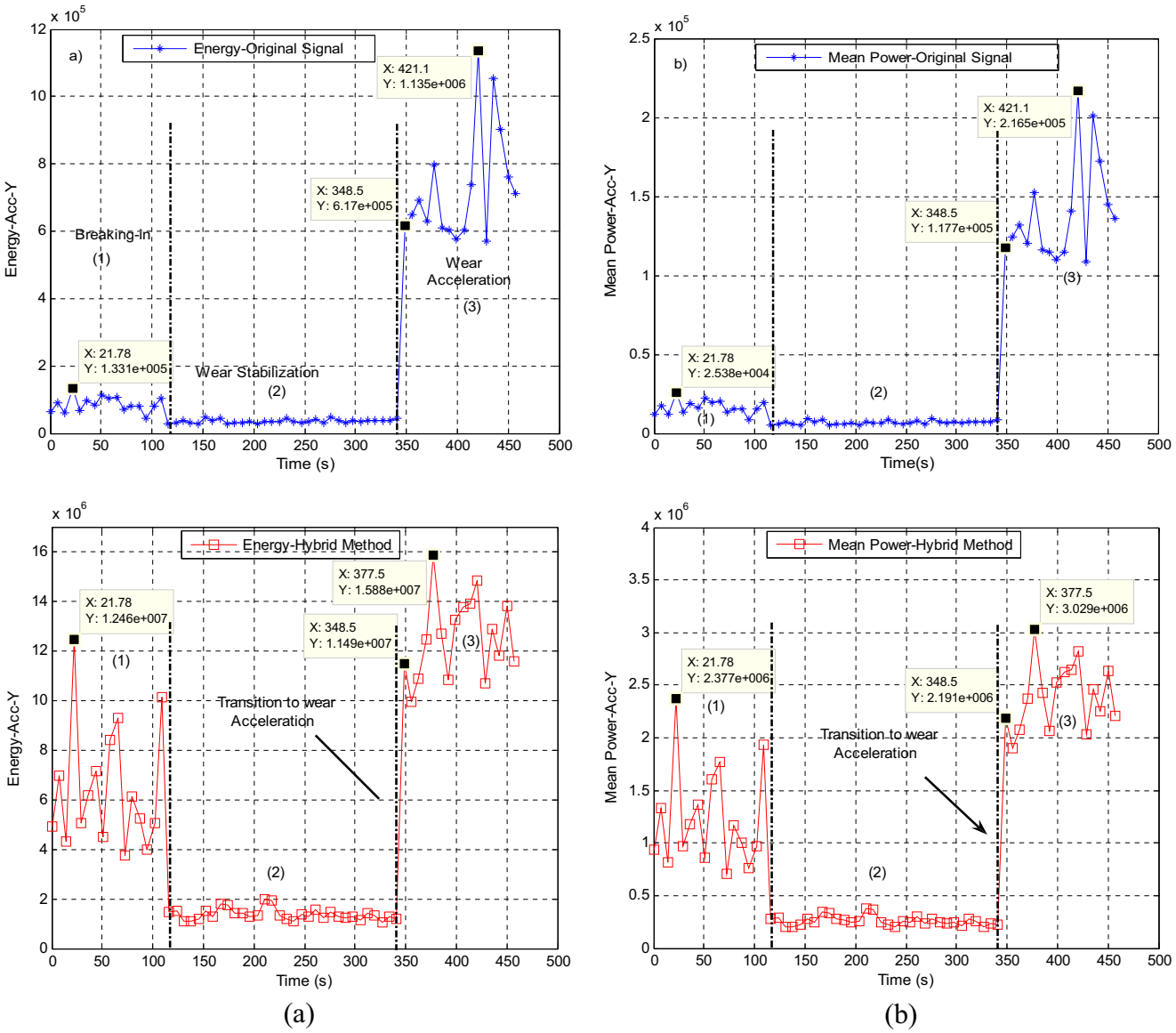

(a) (b)

Fig. 15 Evolution of the scalar indicators (energy and mean power) for the original signal and the reconstructed signal obtained from the proposed hybrid method at V_c=250 m/min; f=0.12 mm/rev; a_p=0.2 mm. **a** Energy, **b** mean power

have then been analysed using wavelet multi-resolution analysis and the empirical mode decomposition alone, and using a proposed hybrid method WMRA/EMD. Two scalar indicators, the energy and the mean power, were used to optimize the proposed method and to evaluate the obtained results.

First, it is to be noted that the vibratory signature in the radial direction is the most significant for wear study; moreover it is very sensitive to the cutting conditions. The most distinguished wear phenomenon is abrasion that appears by grooving on the tool flank face.

Using the scalar indicators, the two components of the proposed method, namely the WMRA and the EMD are optimized. An optimal choice of the WMRA's decomposition vector and the best representative IMF resulting from the EMD has been performed. The results show that the application of the proposed method improve the sensitivity of the used scalar indicators compared to those of the original signal and those obtained from the WMRA and EMD alone. Moreover, the variation of the scalar indicators for the signals obtained from the proposed method allows locating clearly the three wear phases. These phases were not obvious to detect from the original signal.

Acknowledgments This work was achieved in the laboratory LMS (University of Guelma, Algeria). This study received financial support from the Algerian Ministry of Higher Education and Scientific Research (MESRS) and the Delegated Ministry for Scientific Research (MDRS) through CNEPRU Research Project (Code: J0301520130034).

References

1. Kulandaivelu P, Senthil Kumar P, Sundaram S (2013) Wear monitoring of single point cutting tool using acoustic emission techniques. Sadhana 38(2):211–234
2. Mathew MT, Srinivasa Pai P, Rocha LA (2008) An effective sensor for tool wear monitoring in face milling: acoustic emission. Sadhana 33(3):227–233
3. Kuljanic E, Sortino M (2005) TWEM a method based on cutting forces monitoring tool wear in face milling. Mach Tools Manuf 45: 29–34
4. Lim GH (1995) Tool wear monitoring in machine turning. Mater Process Technol 51:25–36
5. Mahfouz IA (2003) Drilling wear detection and classification using vibration signals and artificial neural network. Mach Tools Manuf 43:707–720
6. Mer A, Diniz AE (1994) Correlating tool wear, tool life, surface roughness and tool vibration in finish turning with coated carbide tools. Wear 173:137–144
7. Dimla DE (2002) The correlation of vibration signal features to cutting tool wear in a metal turning operation. Int J Adv Manuf Technol 19:705–713
8. Das S, Roy R, Chattopadhyayal AB (1996) Evaluation of wear of turning carbide inserts using neural networks. Mach Tools Manuf 36:789–797
9. Haili W, Hua S, Ming C, Dejin H (2003) On-line tool breakage monitoring in turning. Mater Process Technol 139:237–242
10. Ravindra HV, Srinivasa YG, Krishnamurthy R (1997) Acoustic emission for tool condition monitoring in metal cutting. Wear 212:78–84
11. Babouri MK, Ouelaa N, Djebala A (2012) Identification de l'évolution de l'usure d'un outil de tournage basée sur l'analyse des efforts de coupe et des vibrations. Rev Sci Technol, Synthèse 24: 123–134
12. Wang L, Mehrabi MG, Kannatey Asibu Jr (2001) Tool wear monitoring in reconfigurable machining systems through wavelet analysis. NAMRI/SME Trans 29:399–406
13. Engin S N, Gülez K A (1999) Wavelet transform artificial neural networks (WT-ANN) based rotating machinery fault diagnostics methodology. Nonlinear Signal and Image Processing NSIP 714–720
14. Mardapittas A S, YHJ Au (2008) Expert system for tool wear monitoring in blanking, Intelligent Fault Diagnosis—Part 1: Classification Based Technique
15. Lei Y, Lin J, He Z, Zuo MJ (2013) A review on empirical mode decomposition in fault diagnosis of rotating machinery. Mech Syst Signal Process 35:108–126
16. Silva RG, Reuben RL, Baker KJ, Wilcox SJ (1998) Tool wear monitoring of turning operations by neural networks and expert system classification of a feature set generated from multiple sensors. Mech Syst Signal Process 12(2):319–332
17. Djebala A, Ouelaa N, Hamzaoui N (2007) Optimisation de l'analyse multirésolution en ondelettes des signaux de chocs. Application aux signaux engendrés par des roulements défectueux. Mécanique Ind 4(8):379–389
18. Mallat S (1989) A theory for multiresolution signal decomposition: the wavelet representation. IEEE Trans Pattern Anal Mach Intell 11(7):674–693
19. Gao Q, Duan C, Fan H, Meng Q (2008) Rotating machine fault diagnosis using empirical mode decomposition. Mech Syst Signal Process 22:1072–1081
20. Liag H, Lin Q, Chen J D Z (2005) Application of the empirical mode decomposition to analysis of Esophageal Manometric Data in gastroesophageal reflux disease, IEEE; 52 (10)
21. Penga ZK, Tsea PW, Chub FL (2005) An improved Hilbert–Huang transform and its application in vibration signal analysis. J Sound Vib 286:187–205
22. Du Q, Yang S (2007) Application of the EMD method in the vibration analysis of ball bearings. Mech Syst Signal Process 21:2634–2644
23. Rilling G. (2007) Décompositions Modales Empiriques: Contributions la théorie, l'algorithme et l'analyse de performances. Ph.D. Thesis, INSA of Lyon, France
24. Huang NE, Shen Z, Long SR, Wu MC, Shih MH, Zheng Q, Yen NC, Tung CC, Liu HH (1998) The empirical mode decomposition and the Hilbert spectrum for nonlinear and non-stationary time series analysis. Proc R Soc Lond 454:903–995
25. Suresh R, Basavarajappa S, Samuel GL (2012) Some studies on hard turning of AISI 4340 steel using multilayer coated carbide tool. Measurement 45:1872–1884
26. Rmili W (2007) Analyse vibratoire pour l'étude de l'usure des outils de coupe en tournage. Thesis, University François Rabelais Tours, France
27. Babouri MK, Ouelaa N, Djebala A (2014) Temporal and frequential analysis of the tools wear evolution. Mechanika 20(2):205–2012